Journal of Applied Fluid Mechanics, Vol. 13, No. 3, pp. 993-1001, 2020.
Available online at www.jafmonline.net, ISSN 1735-3572, EISSN 1735-3645.
DOI: 10.29252/jafm.13.03.30645

Experimental and Numerical Investigation of Friction Coefficient and Wear Volume in the Mixed-Film Lubrication Regime with ZnO Nano-Particle

R. Gholami, H. Ghaemi Kashani, M. Silani and S. Akbarzadeh†

Department of Mechanical Engineering, Isfahan University of Technology, Isfahan, 84156-83111, Iran

†*Corresponding Author Email: s.akbarzadeh@cc.iut.ac.ir*

(Received June 18, 2019; accepted November 4, 2019)

ABSTRACT

One of the most important challenges industry has always been facing is the wear phenomenon. Wear is the cause of huge deteriorations in parts and results in a drop in performance and lifetime of different machines. Therefore, finding solutions to reduce friction coefficient and wear is of special importance. The present research aims at numerical and experimental investigation of friction coefficient and wear in the presence of nano-lubricants. In the numerical section, to tackle different scales of contact components, two sub-models are developed. In the first one, contact of asperities is modeled and the properties of contact surfaces are taken into account. Second sub-model simulates nano-particles in the contact region. Furthermore, a series of experiments are conducted under different loads, speeds, and different values for Zinc Oxide nano-particle weight percent using a pin-on-disk test rig. Results show that predicted friction coefficient and wear volume in theory are reasonably in agreement with experimental results. It was found that adding nanoparticle to the lubricant can be beneficial in terms of friction reduction.

Keywords: Zinc oxide nano-particle; Pin-on-disk test; Nano-lubricant; Wear; Friction coefficient.

NOMENCLATURE

A_{cs}	interference cross sectional area of particle/surface
A_{NP}	contact area for one particle
A_n	nominal area of contact
A_p	contact area of particles
A_s	contact area between surfaces
A_v	void area induced by particles
A_{void}	single particle void area
a	radius of contact
B	the ratio of δ/λ (amplitude/wavelength)
$\boldsymbol{B_c}$	critical value of B
B_{max}	maximum value of B
D_{avg}	average particle size
D	nanoparticle or particle size
d	separation of two surfaces
E'	effective elastic modulus
F_{NP}	particle load
F_c	critical force
F_{ext}	external load
$F_{f,s}$	friction force of the lubricated surface
F_p	external load carried by particles
F_s	external load carried by surfaces
N_{NP}	number of nano-particles in contact
P^*	average contact pressure
R	particles radius
S_y	yield strength
V_{NP}	particle induced wear volume
v	poisson ratio
wt	weight fraction of nanoparticle
a_v	void radius
f_s	friction coefficient for asperities
μ_p	friction coefficient between nano-particles and surfaces
$\boldsymbol{\mu_s}$	friction coefficient of asperities
ρ_{NP}	nano-particle density
ρ_{lub}	lubricant density
ρ_{sol}	nano-lubricant density
σ_g	standard deviation particle
τ_p	shear stress
ω_c	critical indentation
η	nano-particle density
φ	nano-particles distribution
ω	indentation

1. INTRODUCTION

Finding a proper lubricant able to reduce wear and corrosion in every system has attracted special attention these days. Main functions of oil in a tribo-system are lubrication of moving parts, reducing friction and wear, reduction in the generated heat and attracting floating particles and sediments. Since the end users usually expect to have all these advantages at the same time, using a chemical composition consisting of proper additives has been suggested. Sometimes specific additives are used for enhancement of lubricant quality. A variety of additives are treated to motor oils and thus lubricants with various special properties have been introduced to the market. The properties that are reported for commercial additives are heat transfer and stability refinement, reduction of flow obstructions, reducing friction coefficient, reducing wear in motor components, surface repair and surface characteristics refinement, increasing motor life-time and reducing oil consumption and maintenance costs.

Predicting wear for a rigid body moving over a rough surface initiated with Reye's work (1860) which suggested that wear volume is proportional to the work done by friction force. Archard *et al*. (1952) introduced a relation for calculation of adhesive wear called Archard law. This relation states that wear volume is directly proportional to the applied load and distance and inversely proportional to the material hardness. Holm (1967) introduced a theory of atoms interaction for contact between two sliding surfaces and stated the relation between worn particles' volume with applied load and atom detachment probability from surfaces during contact. Investigating wear volume in a mixed lubrication regime, Wang and Wong (2000) showed that change in wear volume and mean asperity height obeys a second order polynomial. Also he studied contact stresses in transition phase of wear considering lubricant effects. Proper equipment was designed and assembled by Akbarzadeh and Khonsari (2011) to study transition phase in wear process. Later in 2016 they studied the validity of applying Miner's rule to adhesive wear prediction under variable and sequential loading. Archard law was investigated in these experiments and it was shown that in sequential loading experiments, Miner's rule was unable to predict the true wear volume. Another case investigated in this experiment was the power loss which was shown to be unique and did not change under different loading.

On the other hand, nano-lubricants have been another topic of interest among researchers. Zhou *et al*. (2000) investigated friction reduction and anti-wear characteristics of Cu nanoparticle as an oil additive using a four-ball machine. The results showed improved tribological properties and load-carrying capacity. The reason introduced was a thin film resulted from chemical reaction. Liu *et al*. (2007) studied tribological properties of nano-lubricants of TiO2, CuO and diamond nano-particles. Their experimental results illustrated that nano-particles especially CuO present good anti-wear and friction reducing properties comparing to the base-oil without any nano-particle. In Battez *et al*. research (2008), where anti-wear behavior of nano-particles was studied, ZnO, CuO and ZrO2 were mixed with base-oil in 0.5, 1 and 1.5 weight percent. They found that all nano-lubricants have less friction coefficient and wear volume than base-oil. Choi *et al*. (2009) studied CuO's tribological behavior in base-oil experimentally using a tribo-meter. They found that average coefficient of friction of this nano-lubricant for 25 nm and 60 nm nano-particles declines 39 and 44 percent respectively. Wu *et al*. (2017) studied wear for TiO2 in water-based lubricants and found 0.8% as the optimized weight fraction of this nanoparticle for the best function in lubricant. So he suggested that water-based nano-lubricants can substantially reduce coefficient of friction (COF).

Most of the researches conducted so far, has concentrated on the experimental study of nano-lubricants. But numerical and FEM modeling of contact have also been attractive fields of study. Polonsky and Keer (1996) presented a new modeling methodology to take into account the scale effect in investigation of micro-contact behavior of asperities. They found that the less the asperities heights, the more difficult the plastic deformation. Jackson (2006) modeled contact of two hypothetical surfaces using stochastic methods and strain gradient modeling. Then, he studied sliding interaction of spheres in an FEM model in 2007. Ghaednia and Jackson (2013) presented an approach to model nano-lubricants. They implemented two sub-models getting the two scales of nano and micro together to predict friction and wear in a nano-lubrication regime. Later Ghednia *et al*. (2016) modeled contact of an elsto-plastic sphere with an elasto-plastic flat to show the effect of their deformation on real force and area of contact. At this year Olsson and Larsson introduced a consistent approach to calculate the force and area of contact between two equal elasto-plastic spheres.

In this paper, the methodology introduced in Ghaenia (2014) has been implemented to predict friction coefficient and wear volume of two contacting surfaces in the presence of nano-lubricant. After validation of the model by pin-on-disk experiments, the effects of nano-paticle weight fraction, load and speed on coefficient of friction and wear volume are discussed in theory and experiments.

2. EXPERIMENTAL INVESTIGATION

A set of experiments has been conducted using the pin-on-disk test rig depicted in Fig. 1. The pin is made of ball-bearing steel 52100 with hardness of 800 Vickers and the disks are made from ST37 rod with hardness of approximately 110 Vickers. Disk properties are described in Table 1.

Table 1 ST37 material properties

Yield Strength	Poisson Ratio	Elastic Modulus	Hardness
150 MPa	0.3	210 GPa	110 Vickers

(a)

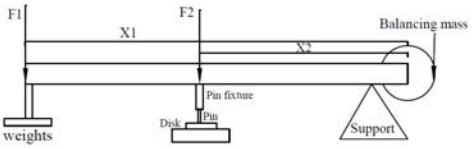

(b)

Fig. 1. (a) Pin on disk test rig, (b) schematic of the device (the load exerted by weights (F1) is converted to the normal load on disk (F2) with the help of distances X1 and X2 (F1*X1=F2*X2)).

The disks have a diameter of 50 mm and thickness of 5 mm and their surfaces are polished to obtain an arithmetic average of asperities as R_a= 0.84 µm. Nano-lubricants are made of 2 components; base-oil and nano-particles. In the present research Sn500 oil is used as the base oil, and ZnO (Zinc oxide) nano-particles with properties as introduced in Table 2 as additives.

Table 2 ZnO nano-particle properties

Color	white
Average Particle Diameter	30-50 nm
Density	5.53 gr/cm^3
Modulus of Elasticity	112.2 GPa
Poisson Ratio	0.336

Table 3 Sn500 oil properties

SAE degree	30
Viscosity at 40°C	107.74 Cst
Density at 15°C	0.8848 gr/cm^3

2.1 Nano-Lubricant Preparation

Since at high weight fractions, the nano-particles might cause abrasive wear, in this study the weight fraction is 0.1-2 % (Ghaednia, 2014). In this case, lubricants of 0.5, 1 and 1.5 percent of Zinc oxide additive and plain lubricant (without any nano-particles) are tested. In order to stabilize the nano-lubricant, mechanical mixer and high-shear mixing were used. This technique helped to get the solution stabilized for longer time (long enough for test performance).

2.2 Pin on Disk Test

To measure the friction coefficient in laboratory, pin-on-disk test rig is used. After nano-lubricant is prepared, the disk is placed inside the fixture and covered by the solution (nano-lubricant). Then, it is adjusted for a specific speed and the load is applied to the upper beam. When the device is switched on, horizontal load transmitted to the pin from disk is measured by the load cell and reported to the computer. Having defined normal load to the system, friction coefficient is measure by dividing the horizontal load on normal load in each point.

To calculate the wear volume, the disk is cleaned by acetone before the experiment and weighed. After each experiment, the disk is precisely cleaned in acetone bath to remove the worn particles and then weighed. The weight difference is reported as the wear weight.

3. SIMULATION

Target system in this research is composed of asperities of two surfaces separated by the lubricant. When surface separation is less than particle diameter, particles are trapped between surfaces. During contact, particles separate surfaces locally which cause void spaces in particles vicinity (Fig. 2). Therefore, the presence of these nano-particles results in change in the real contact area and also the load carried by the particles and subsequently a change in the contact mechanism. Therefore, two different scales are involved in this model. First in the micro scale where contact happens between two rough surfaces depending on asperities' properties, and second in nano scale where particles of nano-size interact with surfaces.

There are two main assumptions in this model. First one is related to statistical nano-particle sub-model where the surfaces inside contact area are assumed flat and the curvature is neglected. Here, a Fourier transformation is implemented to resolve the surface to different sizes defined by a sinus wave (δ-λ in Fig 2).

The second one refers to fluid or lubricant pressure. Lubricant pressure around a nano-particle can alter its deformation and failure. Therefore, the maximum fluid pressure must not exceed contact surface pressure and the worst condition is considered to assess the assumption. Besides, lubricant pressure increase particle hydrostatic stress ending in failure, but not yielding in particles. Multi-scale modeling is helpful here. Accordingly, fluid pressure effect on particles' deformation and failure can be ignored in this study. Moreover, this pressure keeps particles away from pressing each other and postpones their failure. This promotes particles positive effect in contact area (Jackson, 2010).

3.1 Rough Surface Sub-Model

To simulate the contact between rough surfaces, a multi-scale rough surface model was applied (Jackson, 2010). This model is used to decompose

rough surface to sinusoidal waves using Fourier transform. It finds average contact pressure required to overcome all sizes of roughness implementing superposition laws and predicts real area of contact. Equations (1) to (4) represent this model.

$$P^* = \sqrt{2}\pi E' B_{max} \text{ if } B_{max} < B_c \quad (1)$$

$$P^* = \sqrt{2}\pi E' B_{max}\left[\left(\frac{12\pi E' B_{max}}{\sqrt{2}S_y e^{2v/3}} + 7\right)/11\right] \quad \text{if} \quad B_{max} > B_c \quad (2)$$

$$B_c = \frac{\sqrt{2}}{3\pi}\frac{S_y}{E'} e^{2v/3} \quad (3)$$

$$A_s = \frac{F_s}{P^*} \quad (4)$$

Where P^*, E', B, B_{max}, B_c, S_y, v, F_s and A_s are the average contact pressure, the effective elastic modulus, the ratio of δ/λ (amplitude/wavelength) (Jackson, 2010), maximum value of *B*, critical value of B, yield strength, Poisson ratio, force between surfaces and contact area between surfaces, respectively. From Jackson (2010), B is usually around 10E-3 and 10E-4.

3.2 Statistical Nano-Particle Contact Sub-Model

Greenwood and Williamson (GW) originally introduced their model for rough surfaces (Stempflé *et al*. 2010). Height distribution and asperity density considered in original GW model can be accounted for particle size distribution and nano-particle density between surfaces, respectively. Nano-particle density (η) and nano-lubricant density (ρ_{sol}) should be obtained based on practical and measurable parameters.

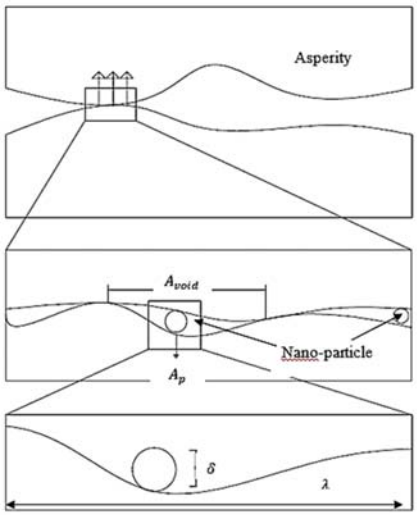

Fig. 2. Scheme of relation between two sub-models; rough surfaces and statistical nano-particle contact.

$$\rho_{sol} = 100\left(\frac{wt\%}{\rho_{NP}} + \frac{100-wt\%}{\rho_{lub}}\right)^{-1} \quad (5)$$

$$\eta(d) = \frac{N_{NP}}{A_n} = \frac{\rho_{sol} wt\% d}{100\rho_{NP}(\frac{\pi}{6}\int_0^\infty \varphi(D)D^3 dD)} \quad (6)$$

Where N_{NP}, A_n, ρ_{NP}, ρ_{lub}, wt, d and D are number of nano-particles in contact, nominal area of contact, nano-particle density, lubricant density, weight fraction of nanoparticle, separation of two surfaces, nanoparticle or particle size. In this research, a normal Gaussian function is assumed for nano-particles distribution (φ).

$$\varphi(D) = \frac{1}{\sigma_g\sqrt{2\pi}} exp\left[-0.5\left(\frac{D-D_{avg}}{\sigma_g}\right)^2\right] \quad (7)$$

Where D_{avg} and σ_g are the average particle size and standard deviation. This statistical sub-model requires a unit nano-particle model to calculate nano-particles change and failure. Spheres under heavy load model were established by Wadwalker *et al.* (2010). This model is introduced assuming elastic deformation and it is assumed that the volume of the sphere is constant. Final equations used for finding particle contact radius are presented in Eqs. (8-12).

$$\left(\frac{a}{R}\right) = \left(\frac{a}{R}\right)_1 + A_1\left(\frac{\omega}{\omega_c}\right)^2 - A_2\left(\frac{\omega}{\omega_c}\right) \quad (8)$$

$$A_1 = 0.0826\left(\frac{S_y}{E'}\right)^{3.148} \quad (9)$$

$$A_2 = 0.3805\left(\frac{S_y}{E'}\right)^{1.545} \quad (10)$$

$$\left(\frac{a}{R}\right)_1 = \sqrt{\frac{\omega}{R}}\left(\frac{\omega}{1.9\omega_c}\right)^{B/2} \quad (11)$$

$$B = 0.14\exp\left(23\frac{S_y}{E'}\right) \quad (12)$$

Where a, R, ω, ω_c are radius of contact, particles radius, indentation, critical indentation, respectively. Contact area for one particle, assuming symmetric contact, is calculated from Eq. (13).

$$A_{NP} = \pi a^2 \quad (13)$$

$$\omega_c = \left(\frac{\pi c S_y}{2E'}\right)^2 R \quad (14)$$

$$c = 1.295\exp(0.73v) \quad (15)$$

Particle load (F_{NP}) is also calculated from Eq. (16).

$$\frac{F_{NP}}{F_C} = \{\exp[-\frac{1}{4}(\frac{\omega}{\omega_c})^{\frac{5}{12}}]\}(\frac{\omega}{\omega_c})^{3/2} + \frac{P}{F_c}\pi R^2(\frac{a}{R})^2 \times \{1-\exp[-\frac{1}{25}(\frac{\omega}{\omega_c})^{\frac{5}{9}}]\} \quad (16)$$

$$\frac{P}{S_y} = 2.84 - 0.92\left[1 - \cos\left(\pi\frac{a}{R_2}\right)\right] \quad (17)$$

$$R_2 = \sqrt{\frac{R^3}{0.76(R-\omega)} - \frac{a^2}{2}} \quad (18)$$

$$F_c = \frac{4}{3}\left(\frac{R}{E'}\right)^2\left(\frac{c}{2}\pi S_y\right)^3 \quad (19)$$

Where F_{NP} is a single particle force and F_c is the critical force.

As previously explained, separation of surfaces by particles cause voids in particles' neighborhood. To estimate radius of void area, half space elastic model was applied. Therefore, the area of this void is calculated by Eq. (20) (Fig. 3).

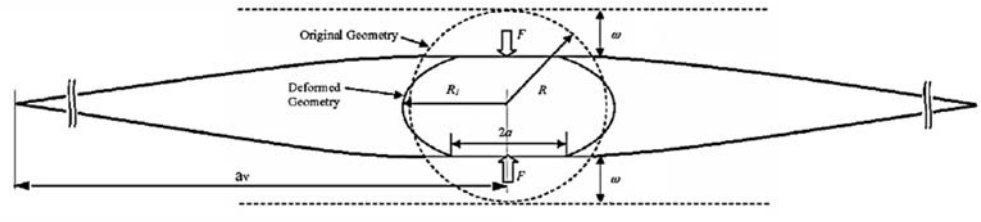

Fig. 3. Schematic representation of spherical particles contact mechanism.

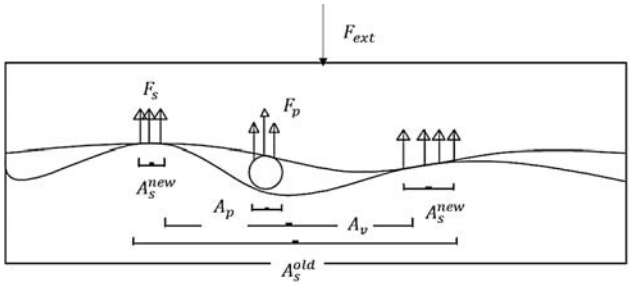

Fig. 4. Schematic representation of surfaces and nano-particles contact.

Resetting and replacing all these parameters in Greenwood-Williamson (GW) represents the final form of statistical nano-particle model shown in Eqs. (21-23) (Greenwood and Williamson, 1966). Here, composite Simpson method has been used for integration.

$$A_{void} = \pi a_v^2 \tag{20}$$

$$\frac{A_p(d)}{A_n} = \int_d^{\infty} \eta(y)\varphi(y)A_{NP}(\omega, D)dy \tag{21}$$

$$\frac{F_p(d)}{E'A_n} = \int_d^{\infty} \eta(y)\varphi(y)\frac{F_{NP}(\omega, D)}{E'}dy \tag{22}$$

$$\frac{A_v(d)}{A_n} = \int_d^{\infty} \eta(y)\varphi(y)A_{void}(\omega, D)dy \tag{23}$$

$$\omega = \frac{y - d}{2} \tag{24}$$

Where A_{void}, a_v, A_p, F_p and A_v are single particle void area, void radius, contact area of particles, force carried by particles and void area induced by particles.

3.3 Algorithm

To solve this case, an algorithm is developed based on the load balancing between two sub-models as shown in Eq. (25). The goal is to determine external load (□□□□) carried by surfaces (□□), external load carried by particles (□□) and investigate force balance equation. First a virtual external load is applied on the system and it is assumed that the total load is carried by the surfaces. Then to find P^* and A_s, rough surface sub-model is used. Assuming that this average pressure is applied to the particles, the load on particles is calculated from Eq. (26). A schematic of contact parameters is depicted in Fig. 4.

$$F_{ext} = F_s + F_p \tag{25}$$

$$F_p = A_s P \tag{26}$$

Note that it is assumed for the particles to be in contact with the surface which means that A_s should be considered as nominal contact area for this statistical model. According to F_p, surface separation (d) and correspondingly A_v and A_p are calculated. Now, contact area is updated through Eq. (27).

$$A_s^{new} = A_s^{old} + A_v \tag{27}$$

Surface force is then updated based on the contact area of surfaces and characterized by Eq. (28). Particles load is also found by equilibrium equation ($F_p = F_{ext} - F_s$) and from statistical sub-model, new A_v and A_p are calculated. Next iterations are solved by reviewing Eq. (27), updating area and repeating the solution. Convergence in this loop is checked by Eq. (29). Final solution is obtained through repeating the loops and checking convergence limit. The whole procedure is summarized in Fig. 5. MATLAB is the programing software implemented in this paper.

$$F_s = A_s P \tag{28}$$

$$\left|\frac{(F_s^{new} - F_s^{old})}{F_s^{old}}\right| < 10^{-3} \tag{29}$$

3.4 Friction Coefficient Calculation

Friction force consists of two terms; friction caused by asperity contact and nano-particles friction related to particles shear stress on the surface.

3.4.1 Friction Coefficient of Asperities

Gelink and Schipper (2000) showed that proportion of shear strength to local normal pressure which is friction coefficient of asperities, has a constant value. Masjedi and Khansari (2014) demonstrated that for an extensive spectrum of surface properties, from extremely smooth to quite rough, friction coefficient for asperities (f_s) is between 0.1-0.13. Therefore,

friction coefficient of asperities is calculated according to Eq. (30).

$$\mu_s = \frac{F_{f,s}}{F_{ext}} = \frac{f_s F_s}{F_{ext}} \tag{30}$$

Where $F_{f,s}$ is the friction force of the lubricated surface. In this research this amount has been assumed 0.12. Also, total normal force F_{ext} and F_s are part of this force which is carried by the surface.

3.4.2 Nano-Particles Friction Coefficient

Friction coefficient between nano-particles and surfaces are calculated using Eq. (31):

$$\mu_p = \frac{A_p \tau_p}{F_{ext}} \tag{31}$$

Looking at these nano-particles hardness, their shear stress (τ_p) is assumed 1.67 GPa (Ohmura *et al.* 2001). Ultimately, to obtain total friction coefficient, Eq. (32) is used.

$$\mu = \mu_s + \mu_p = \frac{f_s F_s}{F_{ext}} + \frac{A_p \tau_p}{F_{ext}} \tag{32}$$

3.5 Calculation of Wear Volume

Combination of particles and surfaces effect to find a general model for wear in this system is challenging. However, based on available statistics, wear can be found from wear models (Williams, 2005).

$$\frac{V_{NP}}{L} = \int_d^{\infty} \eta(y)\varphi(y)A_{cs}(\omega, D)dy \tag{33}$$

$$A_{cs} = \frac{D^2}{8} \{\sin^{-1}[\frac{8\omega(D-\omega)(D-2\omega)}{D^3}] - \frac{8\omega(D-\omega)(D-2\omega)}{D^3}\} \tag{34}$$

Where V_{NP} is particle induced wear volume and A_{cs} is interference cross sectional area of particle/surface.

4. Experimental Results

In this section, the experimental and simulation results are presented and compared. In order to conduct experiments, initially the proper normal loads need to be determined. To this end, first, a load of 20 N was applied to the test device and started working with a velocity of 0.15 m/s. After passing a distance of 1000 m, the wear volume was measured. This test was repeated for 40, 60, 80, 100 and 120 N loads. As represented in Fig. 6, there is a sudden change in the wear volume at the load of 80 N. So the loads slightly lower and slightly higher (60, 80 and 100 N) are selected for the wear experiments.

4.1 Friction Coefficient

The average value of friction coefficient obtained from the experiments is shown in Fig. 7. These experiments are conducted under different applied loads and lubricants with different weight percent of nano-particles.

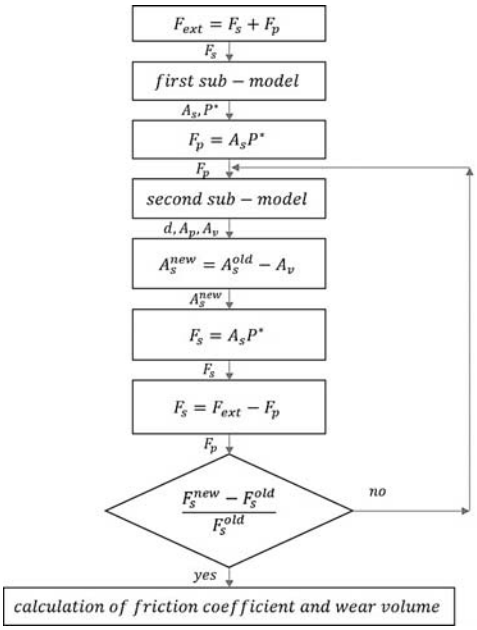

Fig. 5. Flowchart describing solution method.

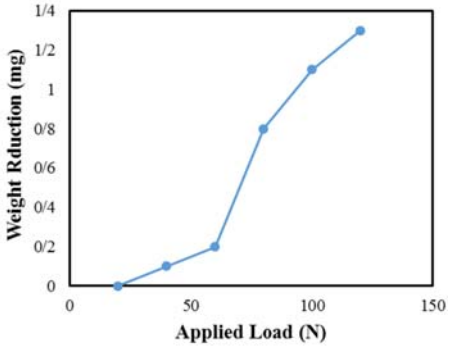

Fig. 6. Wear as a function of load.

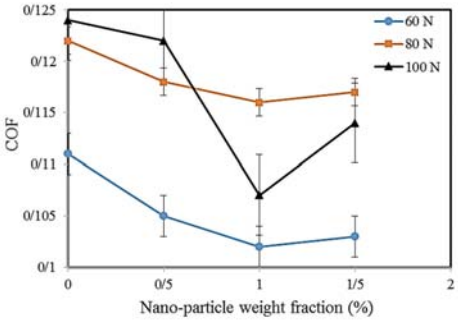

Fig. 7. Friction coefficient as a function of weight percent for different loads in 0.15 m/s.

As illustrated in Fig. 7, by increasing the nano-particles weight percent, friction coefficient reduces for all applied loads and has the least value

in 1% weight. While as the weight percent of nano-particles exceeds 1%, friction coefficient increases.

It can be conferred from this graph that nano-particles presence in the lubricant causes reduction in friction coefficient (Lee *et al*. 2009). The reason is that nano-particles act like nano-ball-bearings and ease the movement of the two contacting surfaces relative to each other. As a result, the friction coefficient decreases. Further increase in the nano-particles result in an increase in the friction coefficient because of nano-particles agglomeration (Wu *et al*. 2018; Xu *et al*. 2019).

4.2 Wear Volume

Figure 8 shows the weight reduction as a function of load and weight percentage. It is observed that as the load is increased, the weight loss increases. It can be concluded that using nano-particles considerably reduce the weight loss. Also, for nano-lubricants the weight loss is the least for 1% weight fraction under all the applied loads.

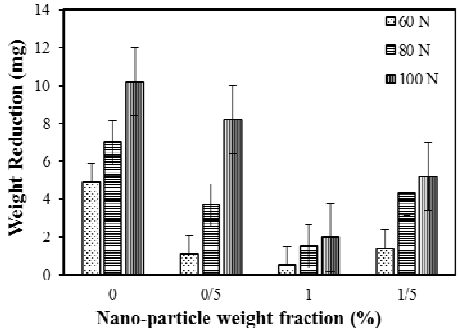

Fig. 8. Comparison of weight loss for different nano-particle weight fractions and different loads under the speed of 0.15 m/s.

In Fig. 9, the effect of adding different weight fractions of nano-particles to the solution is studied under different loads in terms of reduction in weight loss or improvement in weight reduction. The best performance is found for 1% nano-particles in all applied loads.

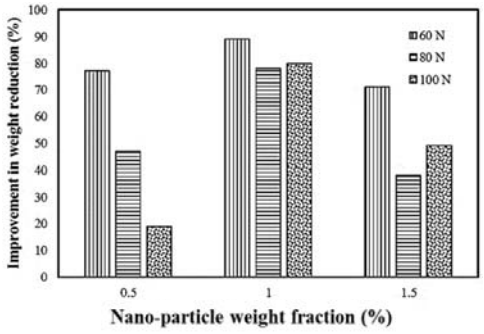

Fig. 9. Improvement in weight reduction compared to raw sample for different normal loads.

4.3 Parametric Study on the Friction Coefficient

Figure 10 shows the effect of sliding speed on the friction coefficient. An increase in the speed results in formation of a thicker lubricant film and therefore the friction coefficient decreases. This behavior is similar to the lubricants without any nano-particles. It is also observed that the minimum friction coefficient occurs in 1% weight fraction.

Figure 11 shows the effect of speed on the weight loss. For all values of weight fractions, the weight loss is higher for 0.1 m/s speed. As the speed increases, a thicker lubricant film is formed and therefore the weight loss decreases. It is observed that for both speeds, the least weight loss corresponds to 1% weight fraction. It is also worthy to note that adding nano-particle to the lubricant results in decrease in the weight loss for all the tested speeds.

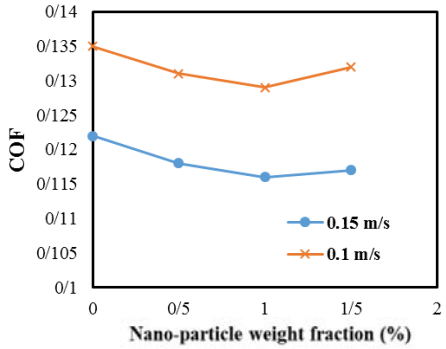

Fig. 10. Friction coefficient as a function of nano-particles weight percent in different speed and under 80 N load.

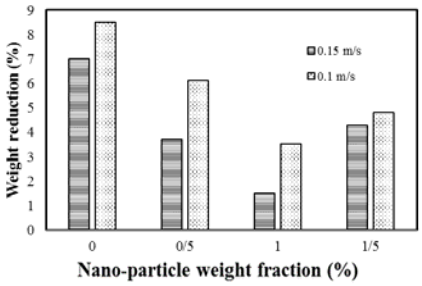

Fig. 11. Reduction in wear volume as a function of nano-particles weight percent for different speeds in a load of 80 N.

5. MODEL VERIFICATION

The results predicted by the proposed model are now verified by comparing to the experimentally-determined results. Both friction coefficient and weight loss are compared in Figs. 12 & 13. Verification proves that this model is more accurate for lower loads

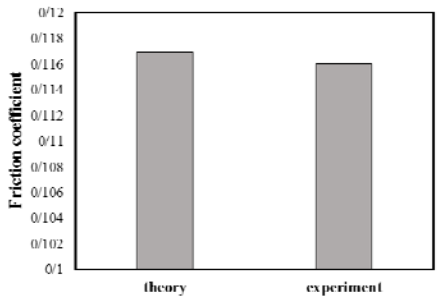

Fig. 12. Comparison between experimental and numerical friction coefficient for 1% weight fraction of nano-particle (load=60 N, speed=0.15m/s).

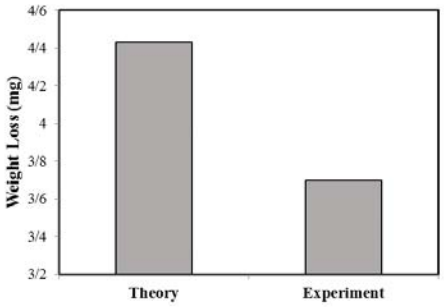

Fig. 13. Comparison between experimental and numerical friction coefficient for 1% weight fraction of nano-particle (load=80 N, speed=0.15m/s).

6. CONCLUSION

In this paper a numerical and experimental study on the effect of adding nano-particles to the base oil is conducted. In experimental section, a set of experiments were conducted by pin-on-disk test rig and in presence of different weight percent of nano-particles. In theory coefficient of friction and wear volume were predicted using a model. To manage multi-scale nature of the problem, two sub-models were implemented. The first one predicts average contact pressure and area of contact. The second predicts the real area of contact for nano-particles, area of voids neighboring the particles, the load on nano-particles and deformation mechanisms of particles. Therefore, in the first step, investigations show good precision in theory fitting the experiment data.

A parametric study on the effect of applied loads, sliding speed, weight fraction of nano-particles on the friction coefficient and wear volume is conducted. The results indicate that adding nano-particles to the base-oil can decrease COF and wear volume and for all applied loads, the best result is obtained for nano-lubricant of 1% volume weight.

ACKNOWLEDGEMENT

The authors would like to thank the financial support of the Iran National Science Foundation (INSF).

REFERENCES

Akbarzadeh, S., and M. M. Khonsari. (2011). Experimental and theoretical investigation of running-in. *Tribology International, 44*(2), 92-100.

Akbarzadeh, S., and M. M. Khonsari. (2016). On the Applicability of Miner's Rule to Adhesive Wear. *Tribology Letters, 63*(2), 29.

Archard, J. F., P. L. Clegg, and A. M. Taylor. (1952). Photoelectric Analysis of Elliptically Polarized Light. *Proceedings of the Physical Society. Section B, 65*(10), 758-768.

Choi, Y., C. Lee, Y. Hwang, M. Park, J. Lee, C. Choi, and M. Jung. (2009). Tribological behavior of copper nanoparticles as additives in oil. *Current Applied Physics, 9*(2), e124-e127.

Gelinck, E. R. M., and D. J. Schipper. (2000). Calculation of Stribeck curves for line contacts. *Tribology International, 33*(3), 175-181.

Ghaednia, H. (2014). *An Analytical and Experimental Investigation of Nanoparticle Lubricants.* Ph. D. thesis, Auburn University, Auburn, Alabama.

Ghaednia, H., and R. L. Jackson. (2013). The Effect of Nanoparticles on the Real Area of Contact, Friction, and Wear. *Journal of Tribology, 135*(4), 603-610.

Ghaednia, H., S. A. Pope, R. L. Jackson, and D. B. Marghitu. (2016). A comprehensive study of the elasto-plastic contact of a sphere and a flat. *Tribology International, 93*(Jan.), 78-90.

Greenwood, J., and J. B. P. P. Williamson. (1966, December). *Contact of Nominally Flat Surfaces.* In Proceedings of the Royal Society of London (A), London, UK.

Hernández Battez, A., R. González, J. L. Viesca, J. E. Fernández, J. M. Díaz Fernández, A. Machado, R. Chou, and J. Riba. (2008). CuO, ZrO2 and ZnO nanoparticles as antiwear additive in oil lubricants. *Wear, 265*(3), 422-428.

Holm, R. (1967). *Electric Contacts*. Springer-Verlag Berlin Heidelberg, Heidelberg, Germany.

Jackson, R. L. (2006). The Effect of Scale-Dependent Hardness on Elasto-Plastic Asperity Contact between Rough Surfaces. *Tribology Transactions, 49*(2), 135-150.

Jackson, R. L. (2010). An Analytical Solution to an Archard-Type Fractal Rough Surface Contact Model AU - Jackson, Robert L. *Tribology Transactions, 53*(4), 543-553.

Jackson, R. L., R. S. Duvvuru, H. Meghani, and M. Mahajan. (2007). An analysis of elasto-plastic sliding spherical asperity interaction. *Wear, 262*(1), 210-219.

Lee, K., Y.-J. Hwang, S. Cheong, Y. Choi, L. Kwon, J. Lee, and S. Kim. (2009). Understanding the

Role of Nanoparticles in Nano-oil Lubrication. *Tribology Letters, 35*, 127-131.

Masjedi, M., and M. M. Khonsari. (2014). Theoretical and experimental investigation of traction coefficient in line-contact EHL of rough surfaces. *Tribology International, 70*, 179-189.

Ohmura, T., K. Tsuzaki, and S. Matsuoka. (2001). Nanohardness measurement of high-purity Fe–C martensite. *Scripta Materialia, 45*(8), 889-894.

Olsson, E., and P. L. Larsson. (2016). A unified model for the contact behaviour between equal and dissimilar elastic–plastic spherical bodies. *International Journal of Solids and Structures, 81*(Mar.), 23-32.

Polonsky, I. A., and L. M. Keer. (1996). Scale Effects of Elastic-Plastic Behavior of Microscopic Asperity Contacts. *Journal of Tribology, 118*(2), 335-340.

Reye, T. (1860). Zur Theorie der Zapfenreibung. *Der Civilingenieur, 4*, 235-255.

Stempflé, P., O. Pantalé, T. Djilali, R. K. Njiwa, X. Bourrat, and J. Takadoum. (2010). Evaluation of the real contact area in three-body dry friction by micro-thermal analysis. *Tribology International, 43*(10), 1794-1805.

Wadwalkar, S. S., R. L. Jackson, and L. Kogut. (2010). A study of the elastic—plastic deformation of heavily deformed spherical contacts. *Proceedings of the Institution of Mechanical Engineers, Part J: Journal of Engineering Tribology, 224*(10), 1091-1102.

Wang, W., and P. L. Wong. (2000). Wear volume determination during running-in for PEHL contacts. *Tribology International, 33*(7), 501-506.

Wang, W., P. L. Wong, and F. Guo. (2004). Application of partial elastohydrodynamic lubrication analysis in dynamic wear study for running-in. *Wear, 257*(7), 823-832.

Williams, J. (2005). *Engineering Tribology*. Cambridge University Press, Cambridge, UK.

Wu, D. (2018). Tribological behaviour of graphene oxide sheets as lubricating additives in bio-oil. *Industrial Lubrication and Tribology, 70*(8), 1396-1401.

Wu, H., J. Zhao, W. Xia, X. Cheng, A. He, J. H. Yun, L. Wang, H. Huang, S. Jiao, L. Huang, S. Zhang, and Z. Jiang. (2017). A study of the tribological behaviour of TiO2 nano-additive water-based lubricants. *Tribology International, 109*(May), 398-408.

Wu, Y. Y., W. C. Tsui, and T. C. Liu. (2007). Experimental analysis of tribological properties of lubricating oils with nanoparticle additives. *Wear, 262*(7), 819-825.

Xu, Y., J. Yu, Y. Dong, T. You, and X. Hu. (2019). Boundary Lubricating Properties of Black Phosphorus Nanosheets in Polyalphaolefin Oil. *Journal of Tribology, 141*(7).

Xu, Y., Q. Zheng, J. Geng, Y. Dong, M. Tian, L. Yao, and K. D. Dearn. (2019). Synergistic effects of electroless piston ring coatings and nano-additives in oil on the friction and wear of a piston ring/cylinder liner pair. *Wear, 422-423*, 201-211.

Zhou, J., Z. Wu, Z. Zhang, W. Liu, and Q. Xue. (2000). Tribological behavior and lubricating mechanism of Cu nanoparticles in oil. *Tribology Letters, 8*(4), 213-218.